

SWIR ASTER band ratios for lithological mapping and mineral exploration: a case study from El Hudi area, southeastern desert, Egypt

A. A. Madani · A. A. Emam

Received: 12 January 2009 / Accepted: 4 May 2009 / Published online: 28 May 2009
© Saudi Society for Geosciences 2009

Abstract This study aims to discriminate and to map the basement rocks as well as the barite mineralization exposed at El Hudi area, Southeastern Desert, Egypt using the processed short-wave infrared bands of advanced space-borne thermal emission and reflection radiometer (ASTER) in collaboration with the field verification and petrographic analysis. El Hudi area is covered dominantly by the Late Precambrian high-grade metamorphic complex of metasedimentary rocks (gneisses, schists, migmatites, and minor amphibolites) which are intruded by the younger granitoids. Nubian sandstones unconformably overlie the basement outcrops and occur as a remnant caps. The metasedimentary rocks cover the area of interest forming a belt of biotite gneisses and migmatites intercalated with hornblende biotite schists and minor amphibolites. Their exposures exhibit well-foliated and banded structures. The metasedimentary rocks have gray and dark gray image signatures on the ASTER band ratio image 8/5, which correspond to biotite gneiss, migmatites, and hornblende biotite schists, respectively. Presence of absorption feature near band 8 (2.295 – 2.365 μm) for the chlorite alteration product is probably responsible for the lowering of the 8/5 band ratio value and the dark gray image signature exhibited by hornblende biotite schists. The granitoid rocks in El Hudi area are late to postorogenic younger granitoids including

three main rock types, Abu Aggag granites, El Hudi garnetiferous muscovite granites, and coarse-grained biotite granites. The acidic dykes are cutting across the granitoids and the gneisses and they form a highly elevated ridges and peaks showing sharp contact with the invaded rocks. Abu Aggag granites are highly dissected by great number of both strike- and dip-slip faults as well as joints trending in NNW–SSE, NNE–SSW, N–S, ENE–WSW, and WNW–ESE directions. On 7/8 band ratio image, Abu Aggag granites have dark gray image signature whereas postgranitic dykes have white image signature. Under the microscope, Abu Aggag granites are homogenous medium to coarse-grained rocks composed mainly of quartz, plagioclase, microcline, and biotite. Zircon, apatite, and opaques are accessories, while chlorite, kaolinite, and epidote are secondary minerals. Presence of absorption feature around band 7 (2.235–2.285 μm) for the kaolinite mineral may be responsible for the dark gray image signature exhibited by Abu Aggag granites. El Hudi garnetiferous muscovite granites are hosting El Hudi barite veins which extend mainly in NNW–SSE and NW–SE. Garnetiferous muscovite granites have gray image signature on 5/4 band ratio image whereas pegmatites and postgranitic dykes have black image signature. Barite veins can be distinguished within garnetiferous muscovite granites by their dark gray image signature on 5/4 band ratio image. The spectral reflectance curve of barite exhibits absorption feature around 2.1 μm (band 5), which leads to lower the ratio value and yields the dark image signature to barite veins. The above-described ASTER band ratio images were integrated into one false-color composite image (8/5:R; 5/4:G; and 7/8:B) which was used to produce 1:100,000 geological map for El Hudi area and to locate the barite mineralization.

A. A. Madani (✉)
Department of Mineral Resources and Rocks,
Faculty of Earth Sciences, King Abdulaziz University,
P.O. Box 80206, Jeddah 21589, Saudi Arabia
e-mail: aamadani18@hotmail.com

A. A. Emam
Geology Department, Aswan Faculty of Science,
South Valley University,
Qena, Egypt

Keywords SWIR ASTER data · Lithologic mapping · Mineral exploration · Band ratio · El Hudi area

Introduction

El Hudi area is a part of Aswan District in the Southern Eastern Desert, Egypt. It is located about 30 km east of Aswan City, between latitudes $23^{\circ} 57'$ and $24^{\circ} 06' 30''$ N and longitudes $33^{\circ} 02'$ and $33^{\circ} 14'$ E (Fig. 1). The area of interest was covered by late Precambrian igneous and metamorphic rocks. Moreover, Nubian sandstone Formation unconformably overlies the basement exposures. Geology of El Hudi area has been an interest research point for several authors, among them: Attia (1955), Zalata (1966), Roufaiel et al. (1976), Ghazaly (1979), Ghazaly (1989), Soliman (1983), El Afandy (1986), Ragab and El-Gharabawi (1985); Ragab and El-Gharabawi (1989), Moghazi et al. (2001), and Fahmy (2007). This study is an attempt to utilize advanced spaceborne thermal emission and reflection radiometer short-wave infrared (ASTER SWIR) images for lithologic discrimination and mapping the late Precambrian igneous and metamorphic rocks, which cover the study area, in addition to locating the barite mineralization.

ASTER is a cooperative effort between the National Aeronautics and Space Administration and Japan's Ministry of Economy Trade and Industry, with the collaboration of scientific and industry organizations in both countries. ASTER captures high spatial resolution data in 14 bands from the visible to the thermal infrared wavelengths and

Table 1 ASTER data characteristics (modified after Fujisada 1995)

| Characteristics | SWIR |
|-------------------|--|
| Spectral range | Band 04 1.600–1.700 μm |
| | Band 05 2.145–2.185 μm |
| | Band 06 2.185–2.225 μm |
| | Band 07 2.235–2.285 μm |
| | Band 08 2.295–2.365 μm |
| | Band 09 2.360–2.430 μm |
| Radiometric | 8 bits |
| Ground resolution | 30 m |
| Swath width | 60 km |

provides stereo viewing capability for digital elevation model creation. The visible near-infrared, SWIR, and thermal infrared wavelength regions of ASTER data provide complementary data for lithologic discrimination and mapping of the alteration products. Table 1 shows the ASTER SWIR data characteristics modified after Fujisada (1995). Throughout this research, ASTER imagery level 1A (AST_L1A.003:2006284127) covering El Hudi area was geometrically corrected to level 1B (UTM projection, zone 36, and datum WGS84) using the geometric coefficients included in the header file within the ERDAS software. Image subsets of the preprocessed ASTER SWIR images for the area of interest were performed for further processing. Several studies dealt with the utilization of ASTER images for lithologic discrimination and detection of alteration products. Qari et al. (2008) utilized the ASTER data for lithologic discrimination of the basement rocks exposed over Arafat area, Western Arabian Shield, Saudi Arabia. They have generated 1:100,000 geological map for the study area using the 6/8, 4/8, and 11/14 band ratio image.

Geologic setting and petrographic analysis

Late Precambrian high-grade metamorphic complex of metasedimentary rocks (gneisses, schists, and minor amphibolites) covers El Hudi area. The younger granitoid rocks intrude these highly deformed and metamorphosed rocks in different parts of study area. Meanwhile, the Nubian sandstones unconformably overlie the basement outcrops and occur as remnant caps. The following paragraphs describe in detail the geologic setting of El Hudi area starting from the older to younger units with their petrographic characteristics.

The metasedimentary rocks represent the oldest rock units and occupy voluminous parts of study area. They form a belt of biotite gneisses and migmatites intercalated with hornblende biotite schists and minor amphibolites.

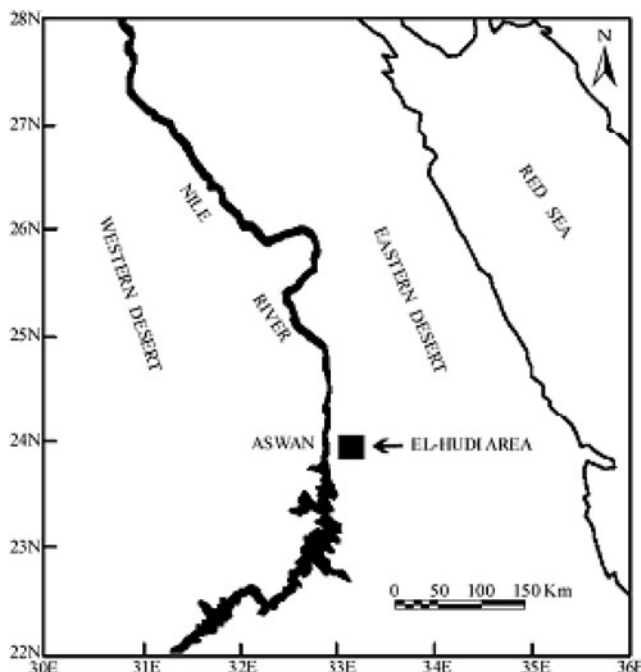


Fig. 1 Location map for the study area

These rocks occupy the central eastern and western parts of El Hudi area. They are fine- to medium-grained and greenish gray to black in color. Their exposures are deeply weathered forming moderate hills and lowlands that exhibit well-foliated and banded structure (Fig. 2a). Moreover, outcrops of these rocks are highly jointed and traversed by two sets of joints nearly perpendicular to each other, giving a pencil-shaped structure (Fig. 2b). The metasedimentary rocks are intruded by the granitoid rocks from the north (Abu Aggag granites), from the south (coarse-grained biotite granites of Khur Um Buweirat), and from the east (El Hudi muscovite leucogranites). A major thrust fault delineates the contact between the metasedimentary rocks and Abu Aggag granite pluton. Both gneisses and granites along this thrust fault are highly deformed and mylonitized over wide zone (Fig. 2c). The schistose rocks are microscopically distinguished into biotite schists and hornblende schists. The biotite schists consist mainly of biotite, quartz, and subordinate plagioclase feldspars, while the hornblende schists are composed essentially of hornblende, quartz, and plagioclase feldspars. Chlorite and epidote are the common secondary minerals.

Granites of Abu Aggag pluton cover voluminous parts (more than 60 km²) in the northern sector of El Hudi area. They are homogeneous (monzo- to syeno-granites) in composition, coarse- to medium-grained, and light pink in color. The pluton has moderate elevation and oval outline. The western and southern margins of Abu Aggag pluton are highly sheared and mylonitized due to effect of thrust fault between the pluton and the metasedimentary belt. Meanwhile, NNW-trending shear zone traverses the western part of this pluton and resulted in highly shearing, fracturing, and jointing of rocks (Fig. 2d). Also, Abu Aggag granites are highly dissected by great number of both strike-slip and dip-slip faults trending in the NNW–SSE, NNE–SSW, N–S, ENE–WSW, and WNW–ESE directions. Figure 2e shows that lateral strike-slip fault traverses Abu Aggag pluton and extends southward through the metasedimentary belt. This fault can be easily delineated from the processed ASTER image (about 9-km length and up to 1-km horizontal displacement). Along the thrust fault zone, these granites are mylonitized showing deformed quartz and feldspar crystals, oriented in parallel alignment within the crushed groundmass with fine biotite flakes. Several acidic to intermediate dykes traverse Abu Aggag pluton in the same above directions. They exhibit various lengths ranging from few meters to few kilometers and thicknesses ranging from few centimeters to tens of meters. Some outcrops of Abu Aggag granites are overlain by Nubian sandstone caps (Fig. 2f). In the eastern part, Nubian sandstone exposures are juxtaposed against Abu Aggag granites directly as a result of dip-slip faulting. The granite and aplite dykes are

numerous in the central, southern, and western parts of El Hudi area. Under the microscope, Abu Aggag granites are homogenous medium to coarse-grained rocks composed mainly of quartz, plagioclase, microcline, and biotite. Zircon, apatite, allanite, and opaques are accessories, while chlorite, sericite (kaolinite), and epidote are secondary minerals.

Remote sensing analysis and interpretation

Band ratio technique is an appropriate technique utilized throughout this study. The ratio images were prepared simply by dividing the DN values of each pixel in one band by the DN values of another band (Drury 1993). Visual inspection of the generated SWIR band ratio images in this study revealed that the most informative images which were used in discrimination and mapping the different rock units covering El Hudi area are: 8/5, 7/8, and 5/4 band ratio images.

The metasedimentary rocks can be easily discriminated on ASTER image 8/5 (Fig. 3a). Biotite gneiss and migmatites have gray image signature whereas hornblende biotite schists have dark gray image signature. Figure 3b shows the spectral reflectance curve of chlorite, the main alteration products of hornblende biotite schists. Presence of absorption feature around band 8 (2.295–2.365 μm) is probably responsible for the lowering of the band ratio value and yields the dark gray image signature to hornblende biotite schists.

Granites of Abu Aggag pluton can be easily discriminated on 7/8 band ratio image (Fig. 3c) in which they have dark gray image signature, whereas the postgranitic dykes have white image signature. Figure 3d shows the spectral curve of kaolinite, the main alteration product of Abu Aggag granites. Presence of absorption feature around band 7 (2.235–2.285 μm) for the kaolinite mineral is probably responsible for the dark gray image signature exhibited by Abu Aggag granites.

The 5/4 ASTER band ratio image for El Hudi barite mineralization mapping

The 5/4 ASTER band ratio image is found to be the best discriminator for El Hudi garnetiferous muscovite granites which host the barite mineralization. El Hudi garnetiferous muscovite granites form moderately elevated lensoidal and elongated bodies that intrude gneisses and schists in the eastern sector of mapped area. The muscovite granites are medium- to coarse-grained massive leucogranites and exhibit light pink color speckled with brownish crystals of garnet. They show sharp contact with their surrounding gneisses and schists (Fig. 4a). These granites are hosting El



Fig. 2 **a** A photograph shows highly foliated low-lying outcrop of hornblende biotite schists, El- Hudi area. **b** A photograph shows pencil-shaped structure in highly foliated and jointed gneiss outcrop, El Hudi area. **c** Thrust fault delineates Abu Aggag granites (*Ag*) and gneisses (*Gn*), El Hudi area. **d** Highly jointed, fractured, and sheared exposure of Abu Aggag pluton located within NNW-trending shear

zone, El Hudi area. **e** A major left-lateral strike-slip fault cuts across Abu Aggag pluton (*Ag*) and extends southward through the metasedimentary belt (*Gn*), El Hudi area. **f** Unconformity surface between Abu Aggag granites (*Ag*) and the overlying Nubian sandstone (*NS*) caps, El Hudi area

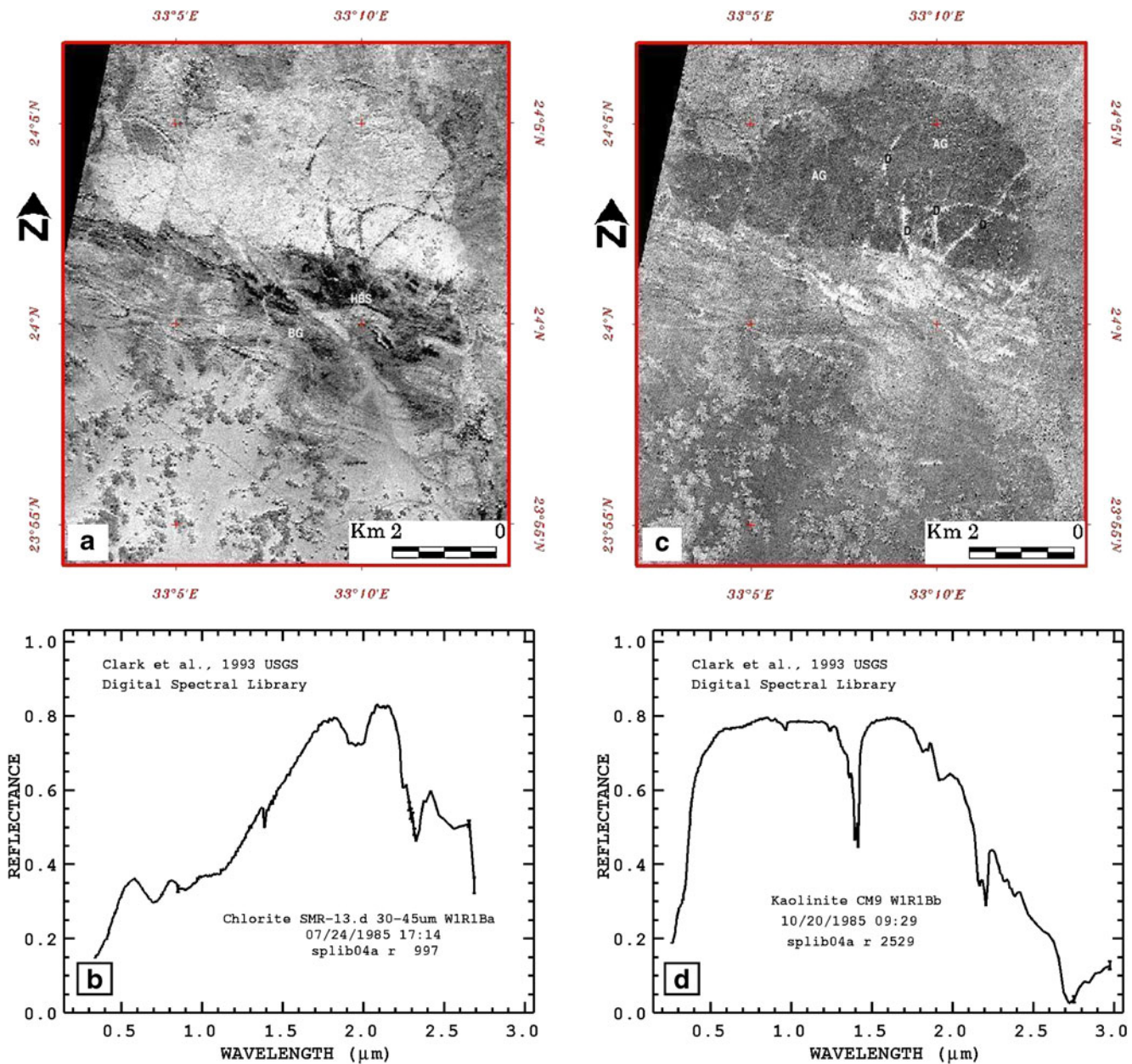


Fig. 3 **a** 8/5 ASTER band ratio image. **b** Spectral curve of chlorite (Clark et al. 1993). **c** 7/8 band ratio image. **d** Spectral curve of kaolinite (Clark et al. 1993)

Hudi barite mineralization, where barite veins extend commonly in NNW–SSE and NW–SE directions and cut across garnetiferous muscovite granite masses (Fig. 4b). NNW-trending shear zone and several strike-slip faults striking NE–SW and ENE–WSW traverse rock masses of muscovite leucogranite. Barite mineralization is located within the NNW-trending shear zone, favoring its hydrothermal origin as fracture fillings. Garnetiferous muscovite granites have gray image signature on 5/4 band ratio image (Fig. 4c) whereas pegmatites and postgranitic rocks have

black image signature. Barite veins can be distinguished within garnetiferous muscovite granites by their dark image signature. Garnetiferous muscovite granites are composed essentially of quartz, k-feldspars, plagioclase, muscovite, minor biotite, and garnet. Zircon, apatite, and opaques are present as accessory minerals, whereas epidote, chlorite, and sericite are secondary minerals. Figure 4d shows the spectral reflectance curve of barite and exhibits absorption feature near $2.1 \mu\text{m}$ (band 5). This means lowering the ratio value and yields the dark image signature to barite vein.

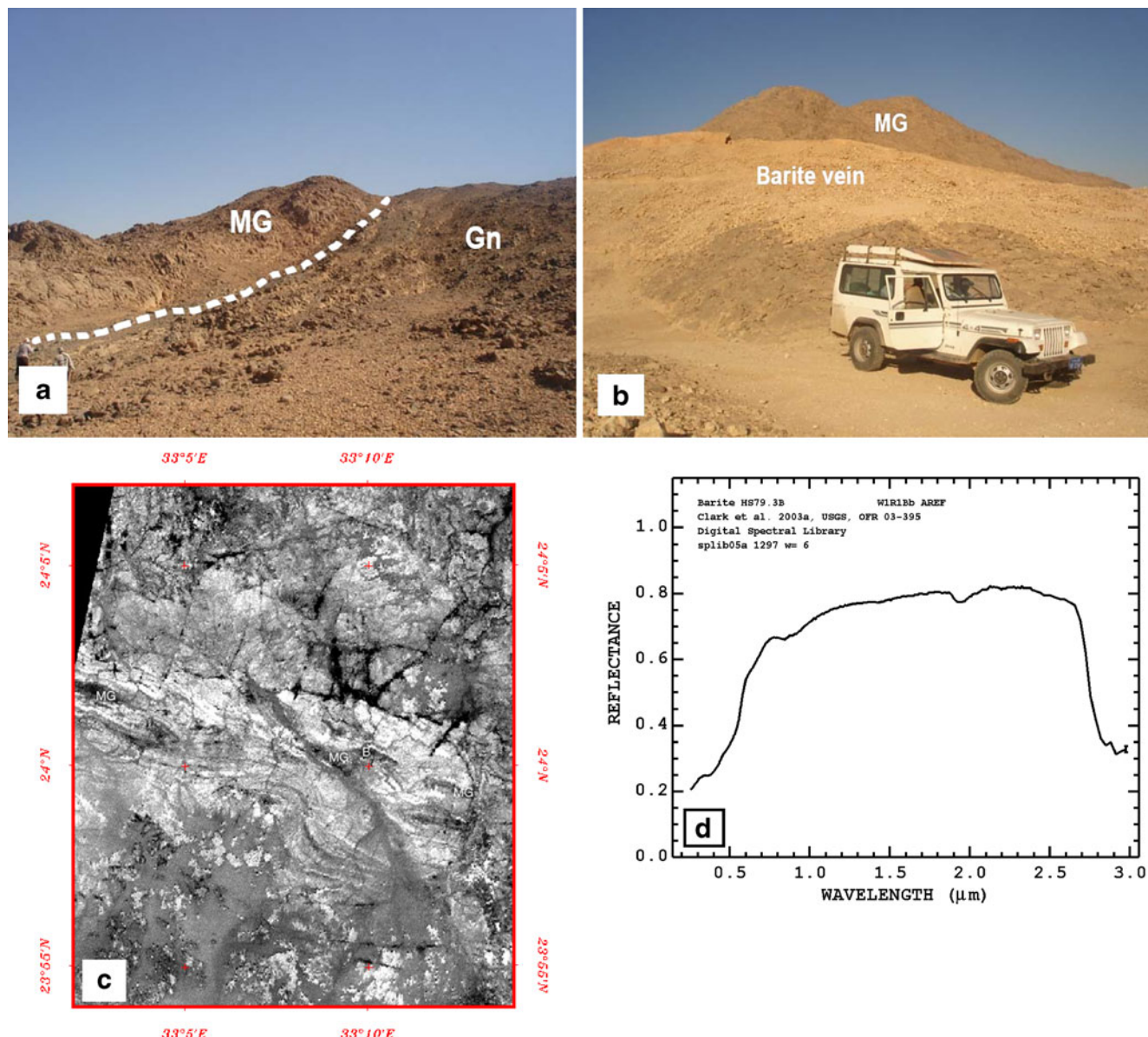


Fig. 4 **a** A photograph illustrates sharp contact between muscovite leucogranites (*MG*) and gneisses (*Gn*), El Hudi area. **b** A photograph shows El Hudi barite mineralization hosted within muscovite

leucogranites (*MG*), El Hudi area. **c** 5/4 band ratio image. **d** Spectral curve of barite (Clark et al. 1993)

Lineaments analysis and barite mineralization

Structurally, faulting and folding are the main controls for the structural pattern of El Hudi area. The fault system shows many tectonic trends, but the predominant trends are in NNW–SSE, WNW–ESE, ENE–WSW, NE–SW, and NW–SE directions. Thrust fault was represented in the study area by El Hudi thrust fault which separates the gneiss schist belt from Abu Aggag granitic pluton. This thrust fault extends mostly in WNW–ESE direction at the south of Abu Aggag pluton and in NNW–SSE direction at the west of pluton. Moreover, folding is represented mainly by the major plunging syncline fold

trending mostly in E–W direction at the central southern part of El Hudi area. The axes of major syncline fold and El Hudi thrust fault are parallel and believed to be related to each other, i.e., generated by the same tectonic phase.

Throughout this study, the authors utilized ASTER panchromatic band 3 for automatic lineaments extraction using the line algorithms of PCI package. The automatically extracted lineaments for the study area are shown in Fig. 5a. Field investigation as well as lineaments analysis revealed that the most common trends cross cutting the metasedimentary rocks are WNW, NW, and NNW whereas the trends NS, NNE, and NE are the common trends

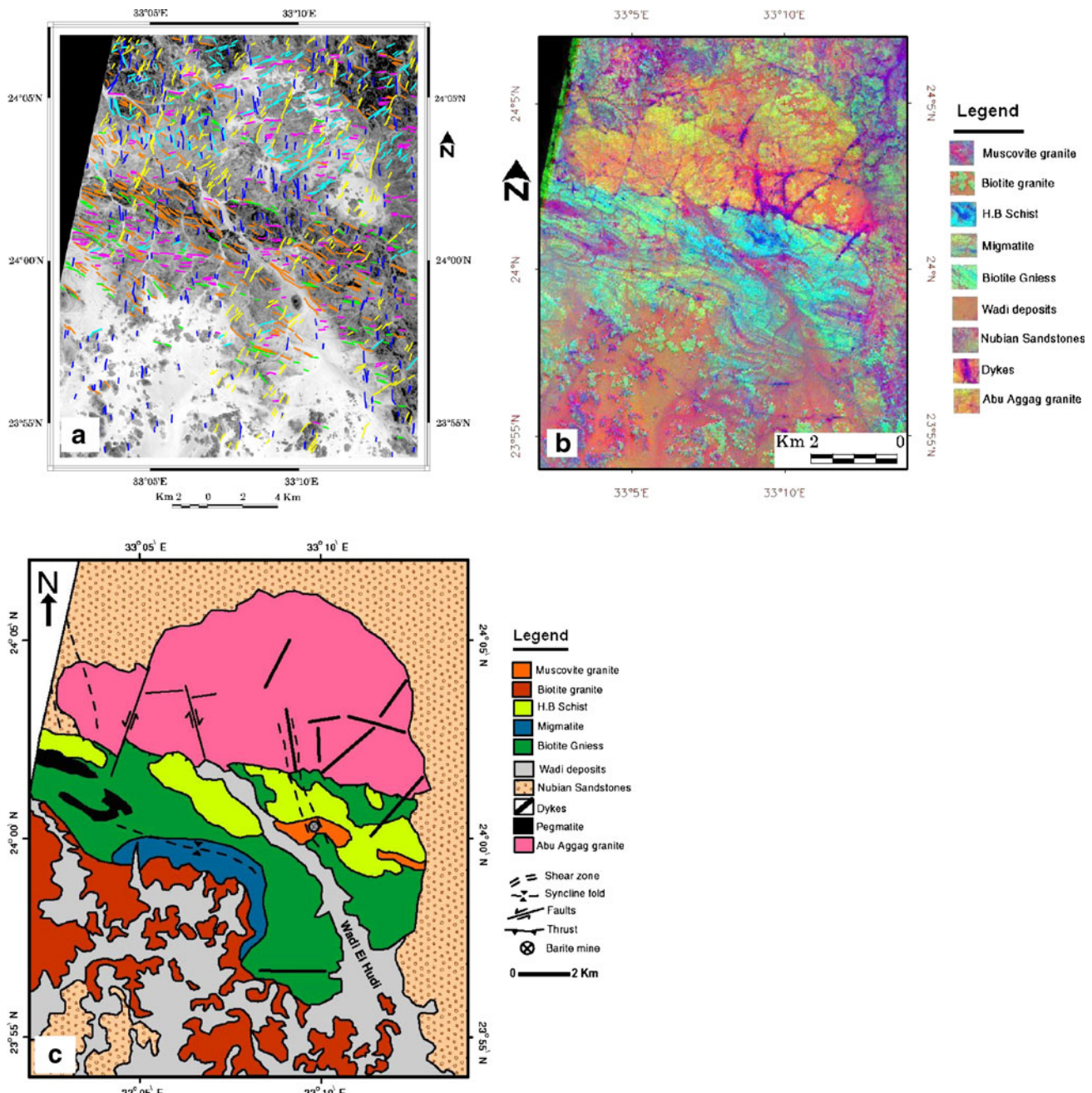


Fig. 5 **a** Lineaments extracted from ASTER band-3 over the study area. **b** FCC ASTER bands ratio image (8/5:R; 5/4G; and 7/8B) for El Hudi area. **c** Geological map for El Hudi area (scale, 1:100,000) generated throughout this study from the processed SWIR ASTER data

dominating in the granitic rocks. The barite veins forming El Hudi barite mineralization are fissure filling located within NNW-trending shear zone cutting across garnetiferous muscovite granites and metasedimentary rocks to the east of El Hudi area. They are structurally controlled and show varying colors from white to brown, depending on the impurities. Most of these veins have been extremely exploited to great depths by making trenches. The veins

are striking predominantly in NNW–SSE and NW–SE directions and steeply dipping to the NE. They have varying lengths from 10 m to several hundreds of meters allowing detection from ASTER data. False-color composite ASTER band ratios image (8/5:R; 5/4G; and 7/8B; Fig. 4b) was generated and combined with the structural information to generate 1:100,000 geological map for El Hudi area (Fig. 5c).

Conclusions

This study is an attempt to utilize the SWIR ASTER band ratio technique in collaboration with field verification and petrographic studies for mapping the Precambrian igneous and metamorphic rocks as well as barite mineralization exposed at El Hudi area. The 8/5, 7/8, and 5/4 ASTER band ratio images were generated and evaluated for mapping the area of interest. The above band ratio images were successfully used to discriminate the metasedimentary granitoid rocks as well as El Hudi garnetiferous muscovite granites which host barite veins. The following conclusions are reached:

1. Biotite gneiss and hornblende biotite schist have gray and dark gray image signatures on 8/5 ASTER band ratio image. Petrographic analysis revealed that the most predominant alteration product is chlorite that has absorption feature around band 8 on its spectral curve. This feature may be responsible for lowering the ratio value and for the dark gray image signature exhibited by hornblende biotite schists.
2. On 7/8 band ratio image, Abu Aggag granites have dark gray image signature, whereas postgranitic dykes have white image signature. This dark gray signature is attributed to the presence of absorption feature near band 7 (2.235–2.285 μm) for the kaolinite mineral.
3. El Hudi garnetiferous muscovite granites, which host barite veins, was successfully discriminated by 5/4 band ratio image. Barite veins occur as fissure filling located within NNW-trending shear zone crosscutting garnetiferous muscovite granites. Barite exhibits absorption feature near band 5, which may be responsible for the dark image signature of barite mineralization within the gray signature of garnetiferous muscovite granites.
4. Analysis of the lineaments extracted using ASTER band 3 in addition to the field check revealed that:
 - (a) The lineaments trends in the metasedimentary rocks have WNW to E–W and NW directions which may represent foliation, lineation, and banded structures exhibited by the metasedimentary rocks.
 - (b) Abu Aggag granites are highly dissected by great number of both strike- and dip-slip faults as well as joints as indicated by field inspection and automatic lineaments extraction. The predominant lineaments trends are NNW–SSE, NNE–SSW, N–S, ENE–WSW, and WNW–ESE directions.

5. False-color composite ASTER band ratio image (8/5:R; 5/4G; and 7/8B) was generated and combined with the field check and lineaments data interpreted from the processed ASTER image to generate 1:100,000 geological map for El Hudi area.

References

- Attia M (1955) Topography, geology and iron-ore deposits of the district east of Aswan. Egyptian Geological Survey Bulletin. Editions Universitaires d'Egypte, Cairo, pp 1–262
- Clark RN, Swayze GA, Gallagher AJ, King TVV, Calvin WM (1993) The U.S. Geological Survey, Digital Spectral Library: version 1: 0.2 to 3.0 microns: U.S. Geological Survey Open File Report 93–592, pp 1340
- Drury S (1993) Image interpretation in geology, 2nd edn. Chapman and Hall, London
- El Afandy AH (1986) Geological studies and radiometric investigations of El Hudi area, Southeast of Aswan, Egypt. M.Sc. Thesis, Ass. Univ., Egypt.
- Fahmy MA (2007) Genesis and mineralogy of pegmatitic rocks in El Hudi and Um Hibal areas, Southeastern Desert, Egypt. M. Sc. Thesis, Aswan Fac Sci., 197 p.
- Fujisada H (1995) Design and Performance of ASTER Instrument. Proc SPIE Int Soc Opt Eng 2583:16–25
- Ghazaly M (1989) Petrochemistry and metamorphic history of El Hudi gneiss complex, East of Aswan. Egypt Egypt Miner J 1:95–109
- Ghazaly MK (1979) Geology of the Hudi area, East of Aswan, Egypt. M.Sc. Thesis, Assu. Univ., Egypt.
- Moghazi AM, Hassanen MA, Hashad MH, Mohamed FH (2001) Garnet-bearing leucogranite in the El Hudi area, southern Egypt: evidence of crustal anatexis during Pan-African low pressure regional metamorphism. J Afr Earth Sci 33:245–259
- Qari M, Madani A, Matsah M, Hamimi Z (2008) Utilization of Aster and Landsat data in geologic mapping of basement rocks of Arafat Area, Saudi Arabia. Arabian J Sci Eng 33(1C):99–116
- Ragab AI, El-Gharabawi RI (1985) Geology and petrology of migmatites, Wadi El Hudi area, East of Aswan, Egypt. Twenty Third Annual Meeting, Egypt J Geol (Abstract)
- Ragab AI, El-Gharbawi RI (1989) Wadi El- Hudi migmatites, east of Aswan, Egypt: a geological study and some geotectonic implications for the Eastern Desert of Egypt. Precambrian Res 44:67–79
- Roufaiel GS, Hilmy ME, Awad NT (1976) Mineralization and geochemical features of the Hudi Barite deposits. Egypt Bull NRC Egypt 1:91–105
- Soliman MA (1983) Petrogenesis of the Hudi batholith and related metamorphic rocks in the district east of Aswan. Egypt J Univ Kuwait (Sci) 10:267–278
- Zalata BA (1966) Geology and mineralogy of pegmatites occurrence at Aswan and Rod El-Biram areas. U.A.R., M.Sc. Thesis, Ain Shams Univ., Egypt